

Article

Experimental and Numerical Study on the Dynamic Thermal Response of Building Interior Decoration Coatings during Intermittent Air-Conditioning in High U-Values Buildings in China

Yanru Li ^{1,*} , Yong Chen ², Lili Zhang ¹ and Xinyi Li ³

¹ College of Architecture and Urban-Rural Planning, Sichuan Agricultural University, Chengdu 625014, China; zlili0720@163.com

² Office of Policy and Regulations, Department of Housing and Urban-Rural Development of Qinghai Province, Xining 810000, China; chenyonghvac@163.com

³ Department of Civil and Structural Engineering, University of Sheffield, Sheffield S10 2TN, UK; amylee_lixinyi@163.com

* Correspondence: li_yanru@163.com

Abstract: Interior decorating coatings (IDCs) are the heat-transfer medium between indoor air and building walls, which mainly form the cooling load and are important in an indoor built environment. To explore the impacts of the precooling process of IDCs on indoor thermal environment of occupants during intermittent air conditioning, this paper investigated the dynamic thermal response of IDCs. Three representative coating materials were integrated to the external insulation wall and internal insulation wall, and their interior surface temperatures were experimentally tested under intermittent air conditioning operation in southern China. Moreover, a heat transfer model was established and verified to analyze the influences of IDC on the thermal response of the interior surface. During the pull-down process, the cold was accumulated in the IDC layer with small thermal diffusivity and could not be transferred into the wall inside, so that the largest temperature reduction was obtained, meaning that the indoor thermal environment could meet the setpoint in a short time. According to modelling calculations, the thick IDC with volumetric specific heat capacity less than $1 \times 10^5 \text{ J}/(\text{m}^3 \cdot \text{K})$ and small thermal conductivity integrated to the internal insulation wall was beneficial to increase the thermal response rate and had the better energy-saving efficiency.

Keywords: interior decoration coating; thermal diffusivity; thermal response; intermittent air-conditioning; indoor thermal environment



Citation: Li, Y.; Chen, Y.; Zhang, L.; Li, X. Experimental and Numerical Study on the Dynamic Thermal Response of Building Interior Decoration Coatings during Intermittent Air-Conditioning in High U-Values Buildings in China. *Energies* **2022**, *15*, 1934. <https://doi.org/10.3390/en15051934>

Academic Editor:
Francesco Minichiello

Received: 4 February 2022

Accepted: 4 March 2022

Published: 7 March 2022

Publisher's Note: MDPI stays neutral with regard to jurisdictional claims in published maps and institutional affiliations.



Copyright: © 2022 by the authors. Licensee MDPI, Basel, Switzerland. This article is an open access article distributed under the terms and conditions of the Creative Commons Attribution (CC BY) license (<https://creativecommons.org/licenses/by/4.0/>).

1. Introduction

Building energy consumption accounted for 46.5% of Chinese total energy consumption in 2018, which was 2.147 billion tce [1]. HVAC systems used to build the indoor environment would further increase the building energy consumption and carbon emissions. The building operation process accounted for 21.9% of the national carbon emissions [1]. Researchers have carried out many optimizations on building envelopes to reduce the energy consumption of HVAC systems [2,3], and also found that intermittent operation of the air conditioner was an effective method [4–6].

The intermittent air conditioning operation is always caused by the occupancy behavior [7,8]. However, the indoor thermal environment of an intermittently air-conditioned house suffers large fluctuations because of the on-off cycling of air-conditioning, resulting in the discomfort of personnel [9]. Unlike continuous air conditioning, the intermittent air conditioning is not able to be considered as steady-state heat transfer, especially in the preheating/precooling stage [10]. The energy used to build the suitable indoor temperature involves a large part of the heat transferred through the building envelope. After turning

on the air conditioner, the time of the indoor thermal environment reaching the setpoint and the energy consumption during this pull-down process are very important. Wang and Lin [11] experimentally studied the influences of different ventilation patterns on energy consumption and thermal comfort during the pull-down process in a typical classroom in Hong Kong. Kulkarni and Hong [12] comparatively studied the thermal comfort in a transient pull-down situation through experiment. Under the intermittent operation, the air-conditioning system needs to offset the transient heat released through the interior surfaces of building envelopes during the pull-down process, which means the building envelope's inner side forms the cooling load, namely precooling. Antonopoulos and Koronaki [13] developed a model to predict the thermal response of indoor air to heat pulses, and used it to carry out optimizations of thermal inertia and selections of wall materials. The thermal response rate of walls under a given temperature step of indoor air depended on the mass and specific heat capacity distributions of the wall's inner side [14]. Wang et al. [6] found that a quick indoor environment increase and less energy consumption could be achieved by choosing the wall materials with small thermal capacity and large heat transfer coefficient. However, the surface temperature of the building envelope was assumed to be equal to the air temperature in the two-stage-lumped parameter model used in their study, which would cause differences from the real situation.

Building envelopes are the interface between indoor and outdoor environments that affect indoor heat loss. The thermophysical properties of building envelopes strongly influence the transient thermal behavior of the building envelope [15]. Many studies focus on optimizing the wall construction under intermittent air-conditioning. Tsilingiris [16] and Meng et al. [5] found that the internal insulation wall with less heat loss was more beneficial to building energy saving than other patterns. However, Barrios et al. [17] comparatively studied the energy consumption during intermittent heating and found that external insulation was more appropriate. Meng et al. [7] found that the average heat transfer could account for 17–22% of the total heat loss under air-conditioning intermittent operation. Li et al. [18] showed that taking advantage of the heat storage and release process of building envelope inside part effectively made the indoor temperature stable after stopping air-conditioning, which could reduce the operation time and be a benefit for energy-saving. The thermal performance design of the building envelope achieves flexibility of energy consumption and indoor thermal environment regulation.

During the intermittent air-conditioning process, the interior decoration coatings (IDCs) are the heat transfer medium between indoor air and building walls, which would directly influence the indoor thermal environment variation and energy consumption. Joudi et al. [19] and Joudi et al. [20] studied the thermal behavior of small cabins with reflective coatings on the interior surface, and found those achieved significant energy savings during both heating and cooling processes. Ibrahim et al. [21] investigated the application of low-E coatings on the wall interior surface by numerical simulation and found that achieved 7–13% energy saving potentials. However, many studies focused on the reflectivity and emissivity of the coatings [22,23], whereas the thermal properties of building materials of the IDCs are ignored. The thermal properties would also affect the thermal performance of IDCs. According to Yoshida et al. [24], the wood decoration employed to the concrete with wood cladding decreased the diurnal variation of the surface temperature and the conductive heat flux.

However, the heat transfer between the indoor air and the building envelope is huge during the pull-down process, which would be affected by the thermal properties of the walls' IDCs, especially the internal heat mass [25]. Research on this subject is hardly found in the literature. Only Meng et al. [26] discovered that IDCs had a significant influence on the temperature and heat flow variations of the interior surface.

During the intermittent air-conditioning, the indoor air temperature variation is due to the coupling heat transfer between the IDCs and the indoor air. Therefore, different thermal performances of IDC materials lead to different dynamic thermal responses, which contributes to the diverse interior surface temperature variation and operative temperature

during the pull-down process. This work focuses on the thermal properties of the IDCs and their impacts on the indoor thermal environment, and aims to find the optimization based on indoor thermal environment regulation during intermittent air conditioning. Through measurements and modelling, the IDCs were investigated and optimized to achieve indoor thermal environment improvement.

2. Methods

An experimental system was set up to study the thermal response of the IDC in Sichuan province, China. The experimental chamber with the size of 3.5 m (length) \times 3.0 m (width) \times 2.2 m (height) was equipped with a split air conditioning unit to achieve intermittent air-conditioning, as shown in Figure 1. Even with the same indoor air temperature variation, the thermal response of the IDC directly influences the indoor thermal environment during the pull-down process [27]. Therefore, to investigate the impacts of IDCs on the dynamic thermal response of building envelope interior surface, the external insulation wall and internal insulation wall in this chamber were tested. These two kinds of walls came from engineering practice in southern China, and their thermal performances were determined by Chinese Standard JGJ 134-2010 [28]. The thermal properties of wall materials are presented in Table 1, and the wall materials are common choices in the building application in Hot Summer and Cold Winter zone in China [29]. Typical IDC materials, including boards, wall decoration and wallpaper et al. [30], were studied, which were aluminum sheet (Al sheet), wall fabric, and wallpaper respectively. The IDCs of the same size (400 mm \times 400 mm) were integrated to both the external insulation wall and the internal insulation wall at the same height. Also, the interior surface temperature of the uncovered wall was tested as the reference. The thermal properties of the IDCs were shown in Table 2. Whereas, thermal resistance, HCA and thermal diffusivity were calculated by Equations (1)–(3). These three parameters could provide explanations of the influence of IDC materials on the wall interior surface temperature. Among them, thermal resistance determines the heat insulation property of the IDC. The higher the thermal resistance, the less heat is transferred through the IDC. HCA represents the heat storage or release amounts per unit area of the IDC when the temperature increases or decreases by 1 °C, indicating the heat or cold storage capacity of the IDC. The value of HCA shows the thermal mass of the internal partitions because of the IDC. Thermal diffusivity describes the rate at which heat flowed from the interior surface to the wall inside, which is related to the speed to reach thermal equilibrium under a variable indoor thermal environment. The low value of thermal diffusivity means that the IDC reduce the possibility that the heat can be transferred into the depth of the wall, resulting in great interior surface temperature reduction. The wall fabric with the biggest HCA has better cold storage capacity during the pull-down process, and its smallest thermal diffusivity indicates that the heat would be accumulated on the interior surface because less heat is transferred into the wall under the same temperature gradient. The heat is quickly diffused from the interior surface of the Al sheet to the wall inside due to the biggest thermal diffusivity.

$$R = \frac{\delta}{\lambda} \quad (1)$$

$$HCA = \rho \times C \times \delta \quad (2)$$

$$\alpha = \frac{\lambda}{\rho C} \quad (3)$$

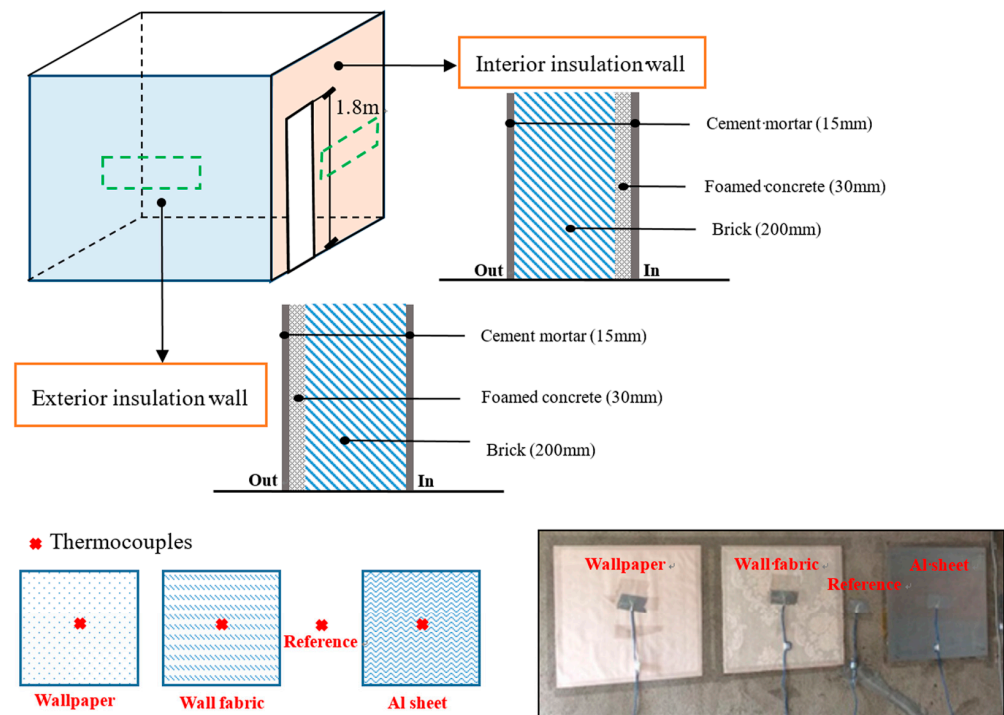


Figure 1. The experimental system.

Table 1. Physical properties of wall layers.

Material	Thickness, m	Density, kg/m ³	Thermal Conductivity, W/(m·K)	Specific Heat, kJ/kg·K	U-Value, W/(m ² ·K)
Cement mortar	0.015	1406	0.35	1.05	
Brick	0.2	1536	0.75	0.523	1.156
Foamed concrete	0.03	104.5	0.087	1.05	

Table 2. Physical properties of IDCs.

Material	Density, kg/m ³	Specific Heat Capacity (J/(kg·K))	Thermal Conductivity, W/(m·K)	Thickness, m	Thermal Resistance, m ² ·K/W	HCA, J/m ⁻² K ⁻¹	Thermal Diffusivity, m ² /s
Al sheet ¹	2710	840	202.77	0.001	4.93×10^{-6}	2276.4	8.9×10^{-5}
Wall fabric ²	1300	1510	0.22	0.0015	0.0068	2944.5	1.1×10^{-7}
Wallpaper ³	700	1469	0.17	0.0005	0.0029	514.15	1.7×10^{-7}

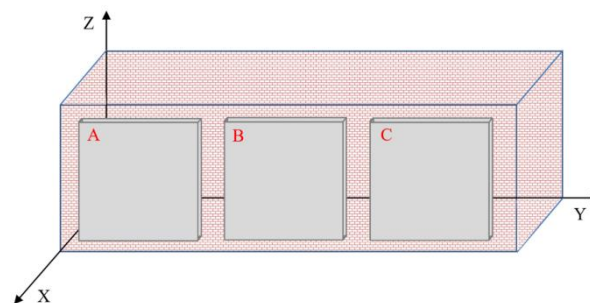
¹ The U-value of the wall decorated with Al sheet is 1.156 W/(m²·K). ² The U-value of the wall decorated with Wall fabric is 1.147 W/(m²·K). ³ The U-value of the wall decorated with Wallpaper is 1.152 W/(m²·K).

Thermocouples and a data logger were used in the experiment; their measurement ranges and accuracies are shown in Table 3. All the thermocouples were calibrated in a 0 °C water bath before the measurement. The thermal responses of different IDCs integrated to two kinds of walls were tested during intermittent air-conditioning. The surface temperatures of three IDCs were measured. The sensors were attached in the center of the interior surfaces (Figure 1). Additionally, the indoor and outdoor air temperatures were recorded. The air conditioning system operated from 7:00 to 11:00 and 13:00 to 17:00 to realize intermittent air conditioning operation. The indoor air temperature was set to a constant value of 22 °C. The operation lasted for three days from 14 July 2016 to 16 July 2016, and the measured data with a test interval of 1 min of the third day were chosen for analysis to eliminate the impact of the wall heat storage on the thermal response in the initial state.

Table 3. The measurement ranges and accuracies of the used instruments and sensors.

Description	Instruments	Range	Accuracy
JTRG-II		−20–100 °C; 0–2000 W/m ²	±0.5 °C, ±5%
T-type thermocouple		−200–350 °C	±0.5 °C

During the measurements, although the horizontal intervals between IDCs were 5 mm, the one-dimensional heat transfer in the test area needed to be verified. Thus, a physical model of the three-dimensional heat transfer process was established. Figure 2 shows the physical model of the building envelope integrated with IDCs. A, B, C in the model present the Al sheet, the wall fabric, and the wallpaper, respectively.

**Figure 2.** Physical model of the building envelope integrated with IDCs.

According to energy conservation, the heat transfer of the building envelope could be described by Equation (4).

$$\frac{\partial}{\partial x} \left(\frac{\lambda}{\rho C} \frac{\partial T}{\partial x} \right) + \frac{\partial}{\partial y} \left(\frac{\lambda}{\rho C} \frac{\partial T}{\partial y} \right) + \frac{\partial}{\partial z} \left(\frac{\lambda}{\rho C} \frac{\partial T}{\partial z} \right) = 0 \quad (4)$$

Boundary conditions of the third kind were adopted for the surfaces of $x = 0$ mm and 230 mm. The other sections used adiabatic boundary conditions. The boundary conditions are numerically defined as follows:

$$\text{When } x = 0, -\lambda \frac{\partial T}{\partial x} \Big|_{x=0} = h_{\text{in}}(T_{\text{in}} - T_{\text{l,in}})$$

$$\text{When } x = 230 \text{ mm}, -\lambda \frac{\partial T}{\partial x} \Big|_{x=230\text{mm}} = h_{\text{out}}(T_{\text{out}} - T_{\text{l,out}})$$

$$\text{When } y = 0 \text{ or } 1215 \text{ mm}, -\lambda \frac{\partial T}{\partial y} \Big|_{y=0 \text{ or } 1215\text{mm}} = 0$$

$$\text{When } z = 0 \text{ or } 410 \text{ mm}, -\lambda \frac{\partial T}{\partial z} \Big|_{z=0 \text{ or } 410\text{mm}} = 0$$

where, T_{out} and T_{in} were 45 °C and 22 °C, respectively. h_{out} and h_{in} were 19 W/(m²·K) and 8.7 W/(m²·K), respectively.

Figure 3 depicts the temperature distributions of the interior surfaces. The difference between each isotherm was 0.02 °C, meaning that no temperature difference in most areas of the three IDCs. The center of IDCs, where the thermocouples were arranged, only had heat transfer in the thickness direction of the wall, indicating the one-dimensional heat transfer.

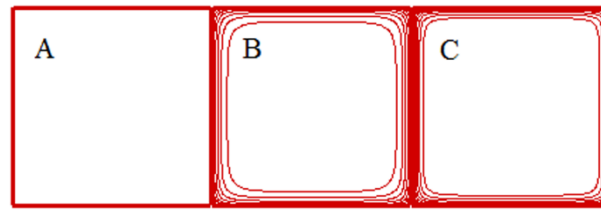


Figure 3. Temperature distributions of the interior surfaces of IDCs.

3. Results

Figure 4 displays the indoor and outdoor air temperature variations. During the daytime, the outdoor air temperature increased due to solar radiation and was at a relatively high value. The maximum outdoor air temperature was 41.8 °C. After 18:00, the outdoor air temperature showed a gradual downward trend. The indoor air temperature decreased slightly during 4:00–7:00 and was about 29 °C. After the air conditioner was turned on at 7:00 and 13:00, the indoor air temperature reduced rapidly. The pull-down process lasted for 50 min. After the air conditioner was turned off at 11:00 and 17:00, the indoor air increased exponentially.

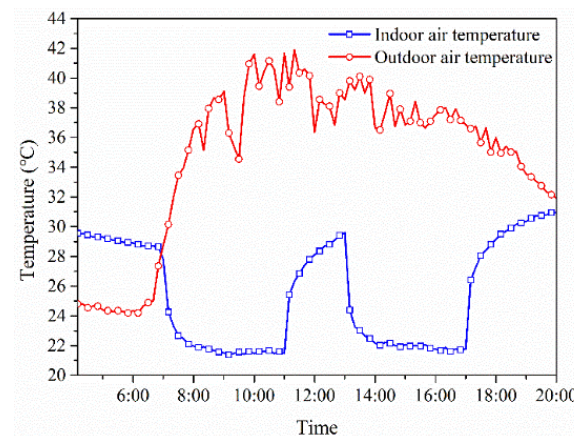


Figure 4. Indoor and outdoor air temperature variations.

Figure 5 shows the interior surface temperature variations of IDCs integrated to the internal insulation wall. Under the initial conditions, the Al sheet had the highest interior surface temperature of 30.2 °C, whereas the wallpaper had the lowest of only 29.6 °C. The interior surface temperatures of IDCs declined after starting air conditioning, and increased when the air conditioner was off, both following exponent laws for two kinds of insulation wall. However, for the internal insulation wall (Figure 5a), the interior surface temperature of three kinds of IDCs elevated because of the heat transferred from the outside into the wall due to the solar radiation from 7:00 to 11:00. The interior surface thermal response rate was calculated through the interior surface temperature changing rate. And the value of IDCs integrated to different walls were similar during the pull-down process, which was wall fabric > wallpaper > Al sheet and were negatively correlated with thermal diffusivity. The thermal diffusivity of the wall fabric was $1.1 \times 10^{-7} \text{ m}^2/\text{s}$, which was the smallest. The cold was accumulated in its IDC layer and could not be transferred into the wall inside during the pull-down process, resulting in the largest temperature reduction, which was more conducive to reaching the required indoor thermal environment quickly. Moreover, the temperature increase rates of wallpaper integrated to both kinds of wall were the largest after turning off the air conditioner. With the largest *HCA*, more cold was stored by the wall fabric compared with the other two IDCs during intermittent air-conditioning. The interior surface temperature of the wall fabric was always lower than the other two IDCs during the first 20–30 min after turning off the air conditioner as its cold was released to the indoor air, which made for maintaining the cool indoor thermal environment.

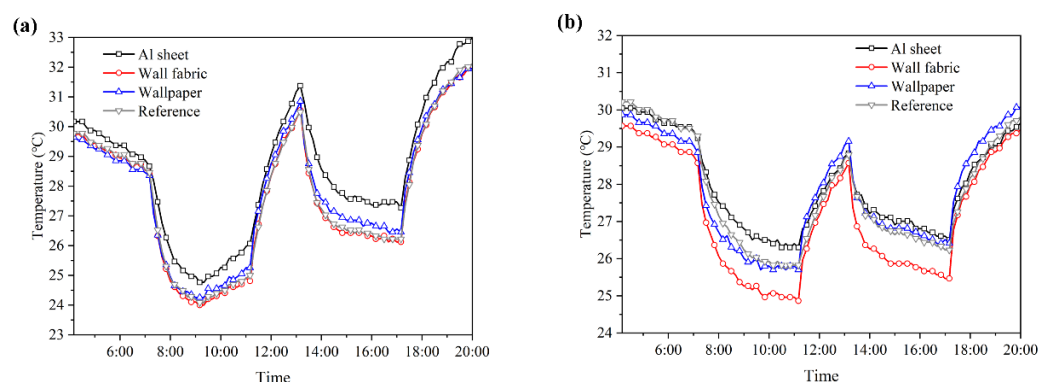


Figure 5. The interior surface temperature variations of IDCs integrated to the same wall ((a) internal insulation wall; (b) external insulation wall).

Figure 6 presents the interior surface temperature variations of the same IDC material integrated to different walls. The thermal response rates of three kinds of IDC materials integrated to the internal insulation wall were all greater than the external insulation wall. Under the first pull-down process (7:00–11:00), the interior surface temperature of the internal insulation wall decreased faster and was always lower than the external insulation wall. The interior surface temperature of Al sheet, wall fabric, and wallpaper integrated to the internal insulation wall could be up to 1.95, 1.36, and 2.06 °C lower than that integrated to the external insulation wall, which would make for building the comfortable indoor thermal environment. After the air conditioner was turned off at 11:00, the interior surface temperature of the internal insulation wall increased rapidly because of the larger thermal response rate, and rose to higher than the external insulation wall after 1 h. The interior surface temperatures of different IDCs integrated to the internal insulation wall were higher than those integrated to the external insulation wall in the initial state of the second pull-down process. Therefore, the surface temperature of the internal insulation wall is higher than that of the external insulation wall for all three kinds of IDCs, even with the greater thermal response rate. Due to the large heat capacity of the wall inside materials of the external insulation wall, much cold storage could be obtained under the pull-down process. Hence, the interior surface temperature of the external insulation wall was more stable than the internal insulation wall, and could maintain the indoor temperature for a long time after stopping air conditioning. Reducing the thermal conductivity of the IDC was beneficial to increase the thermal response rate of the wall interior surface [26]. However, for the internal insulation wall, the insulation layer is close to the wall inside, so the influence of the thermal conductivity of the thin IDC layer on the interior surface thermal response is limited. For the external insulation wall, reducing the thermal conductivity of IDC has a significant effect on increasing the thermal response rate. For the wallpaper and Al sheet integrated to the external insulation wall, the thermal conductivities are 0.17 W/(m·K) and 202.77 W/(m·K), respectively. The thermal response rate of the wallpaper during the first pull-down process was 0.925 °C/h, which was 21.62% higher than the Al sheet. When integrated to the internal insulation wall, the thermal response rate of wallpaper was only 11.36% larger than the Al sheet.

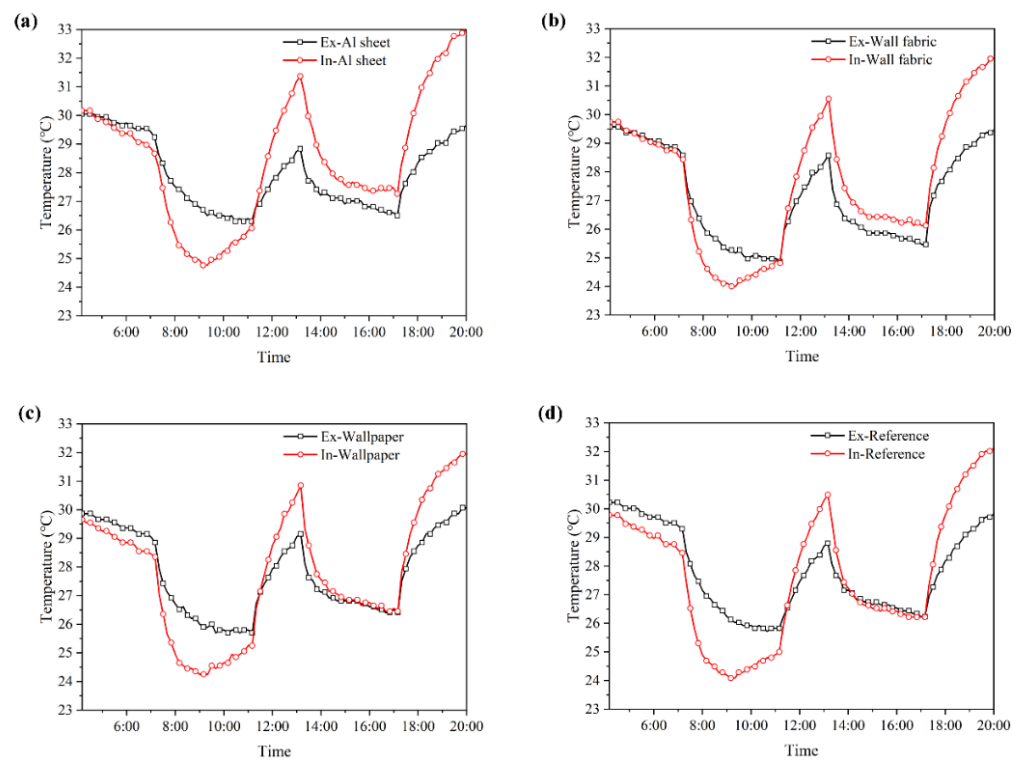


Figure 6. The interior surface temperature variations of the same IDC integrated to different walls ((a) Al sheet; (b) Wall fabric; (c) Wallpaper; (d) Reference).

4. Discussion

When the air conditioning system operates under the intermittent mode, heat is constantly transferred between the indoor air and the building envelope, the IDC act as the mediator between the building envelope and indoor air. To analyze the influence of IDC on the interior surface temperature variations and obtain quantitative influence factors, the most extreme step-way indoor boundary condition was used for calculating. ANSYS-FLUENT was used for analysis. The three-dimensional heat transfer of the wall was simplified to the two-dimensional heat transfer in the thickness and height direction. The two-dimensional heat transfer was described in Equation (5).

$$\frac{\partial T}{\partial \tau} = \frac{\partial}{\partial x} \left(\frac{\lambda}{\rho C} \frac{\partial T}{\partial x} \right) + \frac{\partial}{\partial y} \left(\frac{\lambda}{\rho C} \frac{\partial T}{\partial y} \right) \quad (5)$$

The boundary conditions were:

$$\left\{ \begin{array}{l} \tau = 0 : T = T_0 \\ \tau > 0 \ \& \ x = 0 : -\lambda \frac{\partial T}{\partial x} \Big|_{x=0} = h_{in}(T_{in} - T_{l,in}) \\ \tau > 0 \ \& \ x = \delta : -\lambda \frac{\partial T}{\partial x} \Big|_{x=\delta} = h_{out}(T_{l,out} - T_{out}) \end{array} \right\} \quad (6)$$

The finite volume method was used to discretize the equations of the heat transfer model. A grid-independent solution was tested by using different grid sizes, and the final quantity is 440,000. The test results from measurements were used to verify the heat transfer model. Figure 7 shows the comparison of test values to simulated values. The relative errors of the interior and exterior surface temperatures were less than 5%, indicating that the wall heat transfer model was accurate and could be used for analysis.

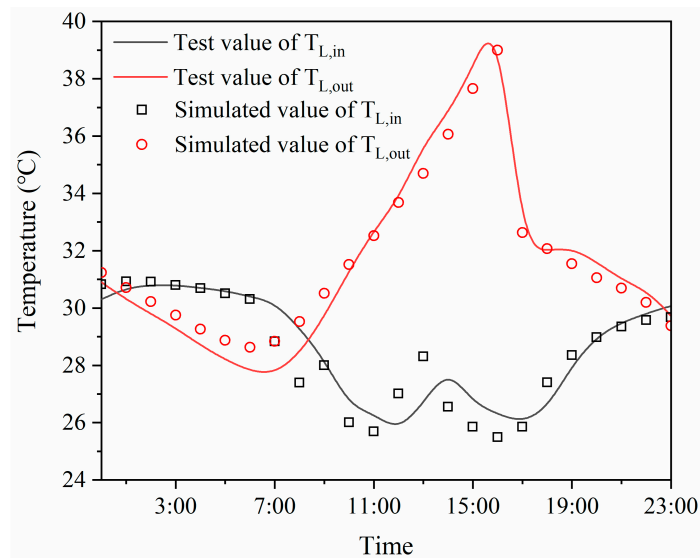


Figure 7. Comparison of test values to simulated values.

During the calculation, the mathematical modelling in this study adopted the following assumptions.

- (1) The initial temperature of the studied system is T_i . In the initial state, when the time $\tau = 0$, $T_{in} = 45$ °C. After starting air conditioning, the indoor air temperature changes stepwise, indicating that when $\tau > 0$, $T_{in} = 22$ °C.
- (2) The outdoor air temperature T_{out} is constant at 45 °C. According to GB 50176-2016 [29], the heat transfer coefficient of the wall interior surface h_{in} and exterior surface h_{out} were set as 8.7 W/(m²·K) and 19 W/(m²·K).
- (3) The heat transfer coefficients of the internal insulation wall and external insulation wall are both 1.38 W/(m²·K).

4.1. Effect on Interior Surface Temperature

Figure 8 presents the interior surface temperature variations for different parameters of the IDCs. With the decrease in the volumetric heat capacity, the interior surface temperature reduction in the internal insulation wall and external insulation wall become great. The impact of the volumetric heat capacity of IDC on the internal insulation wall is more significant than the external insulation wall. Before the volumetric heat capacity increased to 1×10^5 J/(m³·K), increasing the volumetric heat capacity of IDC has little effect on the final surface temperature, but the time constant could be increased and extended by 10 min, which is unfavorable for recovery the indoor thermal environment. The small thermal mass of IDC contributes to reducing the interior surface temperatures and attenuating the operative temperature during the pull-down process. For the thermal conductivity of the IDC, the greater the thermal conductivity, the slower the thermal response rate, and the higher the stable temperature. This phenomenon is also found by Meng et al. [26], and they also claim that the thermal conductivity had the highest energy-saving efficiency. The reason is that when the thermal conductivity of IDC is small, the main construction of the wall directly affects the interior surface temperature. The thermal constant time [6] is mainly affected by the wall brick material when the thermal conductivity of IDC is greater than 0.1 W/(m·K) for the external insulation wall and 10 W/(m·K) for the internal insulation wall. Therefore, increasing the thermal conductivity of IDC has a greater impact on reducing the interior surface temperature of the external insulation wall. The same trend could also be seen in the effect of the thickness of IDC. The large thermal insulation of IDC prevents the heat transferred into the wall, resulting in great temperature reduction in the surface, especially for the external insulation wall with the internal part of high thermal mass. However, for the internal insulation wall, the final stabilization temperature only

differs by 1.4 °C when the thickness is increased by 20 times, and the thermal constant times are all around 600 s. The large heat transfer coefficient enhances the heat exchange between indoor air and the wall interior surface, so that the interior surface temperature decreases quickly, and the stable value is closer to the indoor temperature.

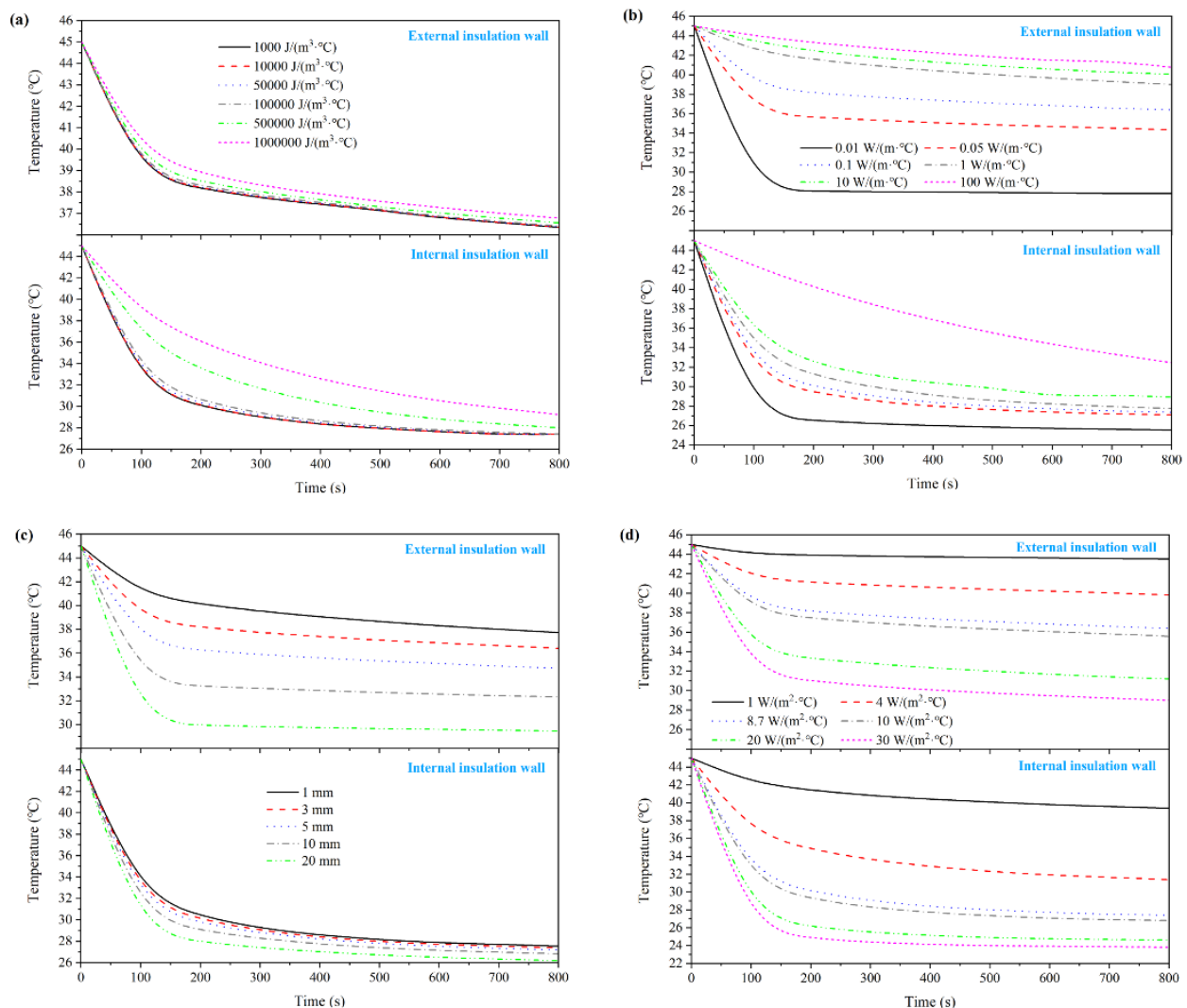


Figure 8. The interior surface temperature variations for different parameters of the IDCs ((a) volumetric heat capacity (b) thermal conductivity; (c) thickness; (d) heat transfer coefficient).

4.2. Effect on the Temperature Reduction in Interior Surfaces

Figure 9 shows the impact of IDC on the interior surface temperature reduction in 20 min pull-down process. It can be also found that the temperature reduction in the internal insulation wall is always greater than that of the external insulation wall, which indicates that the internal insulation wall is more suitable for intermittent air-conditioning. When the thermal conductivity of the IDC is 0.1 W/(m·K), for IDCs with different volumetric heat capacities, the temperature reduction when applying IDC in the internal insulation wall is at least 8 °C larger than the external insulation wall. Figure 9a shows that the temperature reduction declines when the volumetric heat capacity exceeds 1×10^5 J/(m³·K). When the density of IDC is 100 kg/m³, and the volumetric heat capacity is 100 J/(m³·K), the thermal conductivity has a great influence on the surface temperature variations of IDC, shown in Figure 9b. With the increase in thermal conductivity, the surface temperature reduction in both walls decreases significantly. For the internal insulation wall, when the thermal conductivity of IDC is less than 0.1 W/(m·K), the temperature reduction is more

than 18 °C, indicating the large thermal response rate. The thickness of the IDC also has a great influence on the wall interior surface temperature. As can be seen in Figure 9c, the reduction ranges of the interior surface temperatures have increased significantly with the increase in the IDC thickness, especially for the exterior insulation wall. The reason is that the increasing thickness of the IDC causes higher thermal resistance value. Therefore, the cold is resisted to be transferred into the wall and accumulated in the IDC layer, which leads to the large temperature reduction. Figure 9d presents that the surface temperature reductions of two kinds of insulation walls both increase obviously with the increase in heat transfer coefficient. However, the heat transfer coefficient describes the comprehensive impact of the radiative and convective heat transfer on the interior surface of the wall. And the convection heat transfer coefficient depends on the indoor air thermophysical properties and the air velocity [31]. Increasing the convection heat transfer coefficient of the wall interior surface means that an indoor thermal environment is beyond the comfortable range, which is inconsequence. Therefore, to increase the thermal response rate of the interior surface and quickly restore the indoor thermal environment, thick IDCs with small thermal conductivity are preferred.

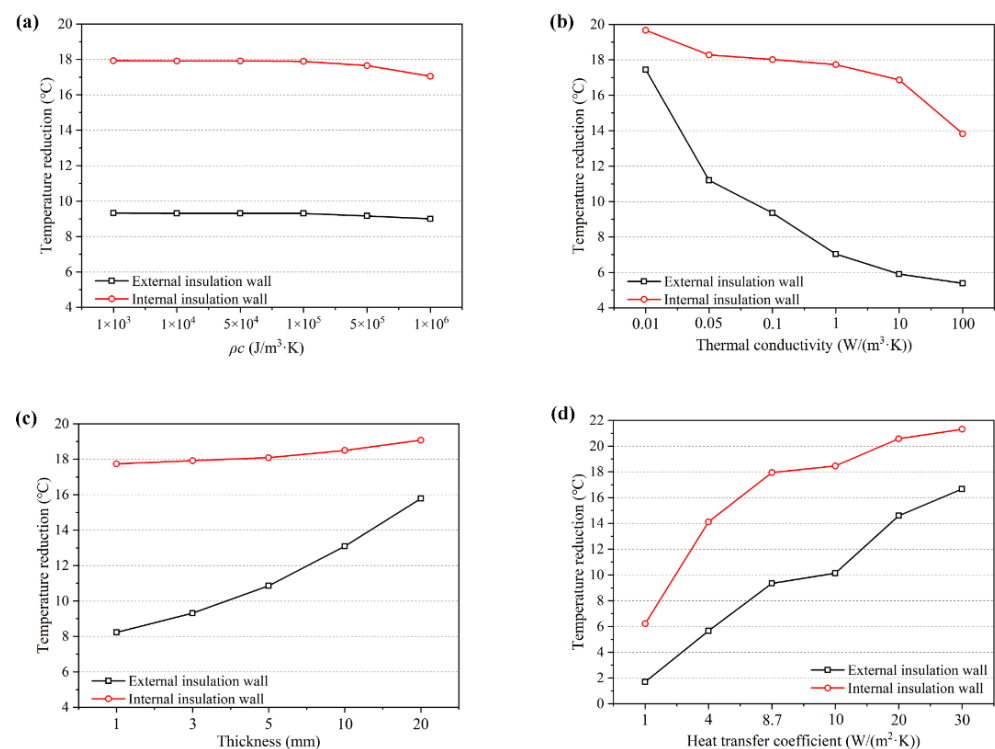


Figure 9. The influence of IDC on the interior surface temperature reduction ((a) volumetric heat capacity (ρc); (b) thermal conductivity; (c) thickness; (d) heat transfer coefficient).

5. Conclusions

In this paper, three representative IDCs were integrated to the internal insulation wall and external insulation wall, respectively, and the thermal responses of their interior surfaces under intermittent air-conditioning operation were experimentally and numerically studied. The main findings of this study are as follows:

- (1) Thermal response rates of the interior surface of the internal insulation wall and external insulation wall met the law of negative correlation with the thermal diffusivity of the IDCs. For the IDC with small thermal diffusivity, the surface temperature was always lower, making the indoor thermal environment more favorable.
- (2) The thermal response rate of the internal insulation wall was greater than that of the external insulation wall after stopping air conditioning. For the external insulation wall, reducing the thermal conductivity of the IDC had a significant effect on increas-

ing the thermal response rate of the interior surface. However, the results could be affected by the choice of stepwise variations of the indoor air temperature.

- (3) Numerical calculation showed that the thick IDC with a volumetric specific heat capacity of less than $1 \times 10^5 \text{ J}/(\text{m}^3 \cdot \text{K})$ and a small thermal conductivity should be preferred to increase the thermal response rate of the interior surface and quickly restore the indoor thermal environment.

This study investigated the thermal response of the IDC affected by the coupling heat transfer under intermittent air conditioning operation, and could contribute to providing energy-saving guidance for the interior decoration design and construction of buildings with intermittent air conditioning. However, due to the simplified boundary conditions in the calculation, the findings were not able to be used for evaluating the indoor thermal comfort conditions. Moreover, the thermal process will also be affected by the thermal emissivity of the IDCs. These will be addressed in future research, as well as the influence on cooling load.

Author Contributions: Conceptualization, Y.C. and Y.L.; methodology, Y.C.; software, Y.C.; validation, Y.L. and L.Z.; formal analysis, Y.L.; investigation, Y.L. and X.L.; resources, L.Z.; writing—original draft preparation, Y.L.; writing—review and editing, X.L. and Y.L.; visualization, Y.L. and L.Z. All authors have read and agreed to the published version of the manuscript.

Funding: This work is supported in part by the scholarship from China Scholarship Council (CSC) under the Grant CSC 202006915024.

Acknowledgments: The authors are grateful to Enshen Long in Sichuan University, who helped with provide the experiment instruments.

Conflicts of Interest: The authors declare no conflict of interest.

Abbreviations

IDC	Interior decoration coating
R	Thermal resistance, $\text{m}^2 \cdot \text{K}/\text{W}$
HCA	Heat capacity, $\text{kJ}/(\text{m}^2 \cdot \text{K})$
ρ	Density, kg/m^3
C	Specific heat capacity, $\text{kJ}/(\text{kg} \cdot \text{K})$
δ	Thickness, m
α	Thermal diffusivity, m^2/s
λ	Thermal conductivity coefficient, $\text{W}/(\text{m} \cdot \text{K})$
τ	Time, s
x	Thickness of the wall unit, m
y	Length of the wall unit, m
z	Height of the wall unit, m
T_{out}	Outdoor air temperature, $^{\circ}\text{C}$
T_{in}	Indoor air temperature, $^{\circ}\text{C}$
$T_{\text{l,out}}$	Exterior surface temperature, $^{\circ}\text{C}$
$T_{\text{l,in}}$	Interior surface temperature, $^{\circ}\text{C}$
h_{out}	Heat transfer coefficients of the exterior surface, $\text{W}/(\text{m}^2 \cdot \text{K})$
h_{in}	Heat transfer coefficients of the interior surface, $\text{W}/(\text{m}^2 \cdot \text{K})$

References

1. China Association of Building Energy Efficiency. *Research Report on Building Energy Consumption in China 2020*; China Association of Building Energy Efficiency: Xiamen, China, 2020.
2. Homod, R.Z.; Almusaed, A.; Almssad, A.; Jaafar, M.K.; Goodarzi, M.; Sahari, K.S.M. Effect of different building envelope materials on thermal comfort and air-conditioning energy savings: A case study in Basra city, Iraq. *J. Energy Storage* **2020**, *34*, 101975. [[CrossRef](#)]
3. Tunçbilek, E.; Arıcı, M.; Krajčik, M.; Nižetić, S.; Karabay, H. Thermal performance based optimization of an office wall containing PCM under intermittent cooling operation. *Appl. Therm. Eng.* **2020**, *179*, 115750. [[CrossRef](#)]

4. Li, Y.; Long, E.; Jin, Z.; Li, J.; Meng, X.; Zhou, J.; Xu, L.; Xiao, D. Heat storage and release characteristics of composite phase change wall under different intermittent heating conditions. *Sci. Technol. Built Environ.* **2018**, *25*, 336–345. [\[CrossRef\]](#)
5. Meng, X.; Luo, T.; Gao, Y.; Zhang, L.; Huang, X.; Hou, C.; Shen, Q.; Long, E. Comparative analysis on thermal performance of different wall insulation forms under the air-conditioning intermittent operation in summer. *Appl. Therm. Eng.* **2018**, *130*, 429–438. [\[CrossRef\]](#)
6. Wang, Z.; Lin, B.; Zhu, Y. Modeling and measurement study on an intermittent heating system of a residence in Cambridgeshire. *Build. Environ.* **2015**, *92*, 380–386. [\[CrossRef\]](#)
7. Meng, X.; Shi, X.; Gao, Y.; Luo, T. Composition of cooling load formed by non-transparent envelopes of a common office building under air-conditioning intermittent operation. *J. Build. Phys.* **2020**, *43*, 528–544. [\[CrossRef\]](#)
8. Gao, Y.; Meng, X.; Shi, X.; Wang, Z.; Long, E.; Gao, W. Optimization on non-transparent envelopes of the typical office rooms with air-conditioning under intermittent operation. *Sol. Energy* **2020**, *201*, 798–809. [\[CrossRef\]](#)
9. Fan, Y.; Toyoshima, M.; Saito, M. Energy conservation and thermal environment analysis of room air conditioner with intermittent supply airflow. *Int. J. Low-Carbon Technol.* **2018**, *13*, 84–91. [\[CrossRef\]](#)
10. Peeters, L.; Van der Veken, J.; Hens, H.; Helsen, L.; D’Haeseleer, W.D. Control of heating systems in residential buildings: Current practice. *Energy Build.* **2008**, *40*, 1446–1455. [\[CrossRef\]](#)
11. Wang, X.; Lin, Z. An experimental investigation into the pull-down performances with different air distributions. *Appl. Therm. Eng.* **2015**, *91*, 151–162. [\[CrossRef\]](#)
12. Kulkarni, M.R.; Hong, F. An experimental technique for thermal comfort comparison in a transient pull down. *Build. Environ.* **2004**, *39*, 189–193. [\[CrossRef\]](#)
13. Antonopoulos, K.A.; Koronaki, I.P. On the dynamic thermal behaviour of indoor spaces. *Appl. Therm. Eng.* **2001**, *21*, 929–940. [\[CrossRef\]](#)
14. Tsilingiris, P.T. On the thermal time constant of structural walls. *Appl. Therm. Eng.* **2004**, *24*, 743–757. [\[CrossRef\]](#)
15. Tsilingiris, P.T. On the transient thermal behaviour of structural walls—the combined effect of time varying solar radiation and ambient temperature. *Renew. Energy* **2002**, *27*, 319–336. [\[CrossRef\]](#)
16. Tsilingiris, P.T. Wall heat loss from intermittently conditioned spaces—The dynamic influence of structural and operational parameters. *Energy Build.* **2006**, *38*, 1022–1031. [\[CrossRef\]](#)
17. Barrios, G.; Huelsz, G.; Rojas, J. Thermal performance of envelope wall/roofs of intermittent air-conditioned rooms. *Appl. Therm. Eng.* **2012**, *40*, 1–7. [\[CrossRef\]](#)
18. Li, Y.; Wang, M.; Zhang, Y.; Long, E. The dynamic thermal process of indoor environment and building envelope during intermittent heating. *Indoor Built Environ.* **2018**, *28*, 422–433. [\[CrossRef\]](#)
19. Joudi, A.; Svedung, H.; Bales, C.; Rönnelid, M. Highly reflective coatings for interior and exterior steel cladding and the energy efficiency of buildings. *Appl. Energy* **2011**, *88*, 4655–4666. [\[CrossRef\]](#)
20. Joudi, A.; Svedung, H.; Cehlin, M.; Rönnelid, M. Reflective coatings for interior and exterior of buildings and improving thermal performance. *Appl. Energy* **2013**, *103*, 562–570. [\[CrossRef\]](#)
21. Ibrahim, M.; Bianco, L.; Ibrahim, O.; Wurtz, E. Low-emissivity coating coupled with aerogel-based plaster for walls’ internal surface application in buildings: Energy saving potential based on thermal comfort assessment. *J. Build. Eng.* **2018**, *18*, 454–466. [\[CrossRef\]](#)
22. Nemli, G.; Örs, Y.; Kalaycıoğlu, H. The choosing of suitable decorative surface coating material types for interior end use applications of particleboard. *Constr. Build. Mater.* **2005**, *19*, 307–312. [\[CrossRef\]](#)
23. Shuba, Y.A.; Sidorovskii, N.V. Reflection indicatrices as basic characteristics of the optical properties of a material. *J. Opt. Technol.* **1998**, *65*, 724–727.
24. Yoshida, A.; Shoho, S.; Kinoshita, S. Evaluation of reduction effect on thermal load inside and outside of concrete building with woden decoration by numerical analysis. *Energy Procedia* **2013**, *132*, 435–440. [\[CrossRef\]](#)
25. Di Perna, C.; Stazi, F.; Casalena, A.U.; D’Orazio, M. Influence of the internal inertia of the building envelope on summertime comfort in buildings with high internal heat loads. *Energy Build.* **2011**, *43*, 200–206. [\[CrossRef\]](#)
26. Meng, X.; Gao, Y.; Yu, H. Effect of inner decoration coating on inner surface temperatures and heat flows under air-conditioning intermittent operation. *Case Stud. Therm. Eng.* **2019**, *14*, 100503. [\[CrossRef\]](#)
27. Fanger, P.O.; Ipsen, B.M.; Langkilde, G.; Olesen, B.W.; Christensen, N.K.; Tanabe, S. Comfort limits for asymmetric thermal radiation. *Energy Build.* **1985**, *8*, 225–236. [\[CrossRef\]](#)
28. Ministry of Housing and Urban-Rural Development. *Design Standard for Energy Efficiency of Residential Buildings in Hot Summer and Cold Winter Zone (JGJ 134-2010)*; China Architecture & Building Press: Beijing, China, 2010.
29. Ministry of Housing and Urban-Rural Development. *Thermal Design Code for Civil Building (GB 50176-2016)*; China Architecture & Building Press: Beijing, China, 2016.
30. Hou, M.; Wang, Y.; Zhao, H.; Zhang, Q.; Xie, Q.; Zhang, X.; Chen, R.; Chen, J. Halogenated flame retardants in building and decoration materials in China: Implications for human exposure via inhalation and dust ingestion. *Chemosphere* **2018**, *203*, 291–299. [\[CrossRef\]](#)
31. Laloui, L.; Rotta Loria, A.F. Chapter 3—Heat and mass transfers in the context of energy geostructures. In *Analysis and Design of Energy Geostructures*; Laloui, L., Rotta Loria, A.F., Eds.; Academic Press: Cambridge, MA, USA, 2020; pp. 69–135.